J Mater Sci: Mater Med (2006) 17:1089–1093
DOI 10.1007/s10856-006-0535-6

The effect of pressure during sintering on the strength and the fracture toughness of hydroxyapatite ceramics

Satoshi Kobayashi · Wataru Kawai · Shuichi Wakayama

Received: 27 June 2005 / Accepted: 14 November 2005

Abstract Hydroxyapatite (HA) is known to be biocompatible and osteoconductive, and can be synthesized chemically. The objective of the present study is to clarify the effect of pressure during sintering on the mechanical properties of HA. HA was sintered using a hot press system at a uniaxial pressure ranging from 7.81 to 62.5 MPa at a maximum temperature of 1200°C with a heating rate of 10°C/min. The density of the HA increased with increasing pressure and peaked at the sintering pressure of 31.2 MPa. Four-points bending tests and fracture toughness measurements with indentation method were conducted to clarify the effect of sintering pressure. Bending strength decreased at the pressure >31.2 MPa. This result indicates that residual stress generated during sintering process became larger with increasing pressure. Fracture toughness were also lower with high density HA.

1 Introduction

Hydroxyapatite (HA), the main mineral constituent of vertebrate skeletal systems, has the approximate chemical composition $Ca_{10}(PO_4)_6(OH)_2$. Synthetic HA is used in hard tissue replacement applications since it is capable of undergoing bonding osteogenesis and is chemically stable for long periods of time *in vivo*. Synthetic HA is simply a fine-grained polycrystalline ceramic and sintering process of HA have been studied. Royer *et al.* [1] investigated the initial composition (Ca/P) of the raw powder on the mechanical properties of sintered body. Halouani *et al.* [2] measured the relative density and average grain size as a function of temperature during hot-pressing. They clarified that a decrease of both strength and toughness was observed with increasing average grain size. Van Landuyt *et al.* [3] investigated the influence of high sintering temperature on the mechanical properties of HA. In their study, nearly theoretical density is achieved at 1300°C and a maximum fracture toughness is obtained for the samples sintered at 1300°C whereas hardness increases up to a sintering temperature of 1400°C. Ruys *et al.* [4] investigated the effect of sintering temperature on the tensile strength, Weibull modulus, density, decomposition, dehydroxylation and microstructure of HA sintered under a 1 MPa purity argon atmosphere. Fanovich and Lopez [5] investigated the effect of temperature and additives on the microstructure and sintering behavior of HA with different Ca/P ratio sintered at the atmospheric pressure. Muralithran and Ramesh [6] also investigated the effect of temperature on the properties of HA. Thangamani *et al.* [7] investigated the effect of powder processing on densification, microstructure and hydroxyapatite. They also investigated the effect of sintering temperature. Guo *et al.* [8] studied the effect of temperature on the microstructure of HA with Rietveld method. Gu *et al.* [9] examine the spark plasma sintering of HA and the effect of temperature on sintering behavior of HA was investigated. As mentioned above, many studies were conducted on the sintering of HA, especially the inestigation of the effect of temperature. On the other hand, there is little study on the pressure condition during sintering process, though the pressure condition as a driving force of the surface and volume diffusion between the particles during sintering is very important factor.

The objective of the present study is to clarify the effect of sintering pressure on the mechanical properties of HA,

S. Kobayashi (✉) · S. Wakayama
Mechanical Engineering Course, Faculty of Urban Liberal Arts, Tokyo Metropolitan University, 1-1 Minami-Osawa, Hchioji, Tokyo 192-0397, Japan
e-mail: koba@ecomp.metro-u.ac.jp

W. Kawai
Under graduate student, Tokyo Metropolitan University

experimentally. HA was sintered at five different pressure conditions using a uniaxial hot press system. The sintered bodies of HA were evaluated using bending and indentation testing.

2 Experimental procedure

A commercially available HA powder (HAP200, Taihei Chemical Co., Japan) was used for all test samples. The HA powders were sintered on a uniaxial hot press (HP-88-CC-23-S, NEMS Co., Japan). 4 sets of 5 g HA powders were placed into the graphite die with a diameter of 20 mm as shown in Fig. 1. The graphite die was set in the furnace of the hot press system and powders were pressurized. In order to investigate the effect of sintering pressure on the mechanical properties of HA, the pressure levels were selected as 7.81 MPa, 15.6 MPa, 31.2 MPa, 46.8 MPa and 62.5 MPa. Then, furnace atmosphere was replaced by high purity argon. The graphite die was heated in the furnace to 800°C at 10°C/min, kept for 1 h and heated again to 1200°C at 10°C/min. Then, the pressure was set to 0 MPa and the die was cooled to room temperature at 10°C/min. The sintering program is shown in Fig. 2. Density measurements based on Archimedes' principle were conducted. Three measurements were conducted on each disk to give the average value.

X-ray diffraction (XRD) analysis was used to characterize the effect of the sintering pressure on the structure of HA with goniometer (M21XHF22-SRA, MacScience, Japan). XRD pattern was obtained with CuKα radiation at 40 kV and 300 mA. The samples were scanned from 10°(2θ) to 80°(2θ) at a scan rate of 1°per min.

In order to characterize the grain size, the surface of the thermally-etched HA was observed with a scanning electron microscope (S-2500CX, Hitachi, Japan). Thermal etching were conducted with a electric furnace (SSF-2030-R,

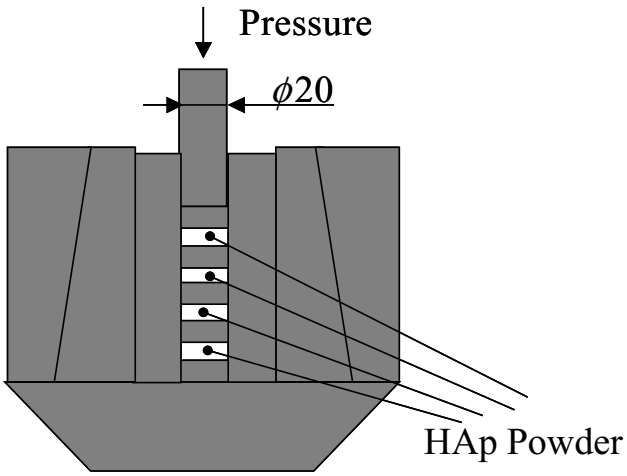

Fig. 1 Schematic view of die set with HA powder.

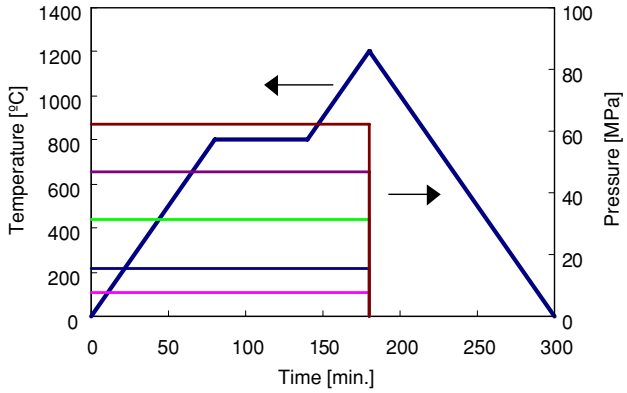

Fig. 2 Sintering program of HA.

Yamada Electric Co., Japan). HA was heated at 50°C/min to 1100°C, kept for 1 h and cooled to room temperature at the furnace.

The sintered compacts were then polished to a 3 μm finish and cut with a diamond resinoid blade (NASTRON TC-2, Heiwa, Japan). The specimen size was 15 × 2 × 1 mm. Tensile surface of the specimen was also polished to a 1 μm finish. The corners were chamfered and also polished to a 1 μm finish. In order to minimize the effect of water content on fracture process, specimens were then dried in vacuum drying oven (DP-23, Yamato Co, Japan) at 150°C for 2 h. More than twenty specimens were prepared for both bending tests and fracture toughness tests at each pressure condition.

Four points bending tests were conducted with an inner span, l, of 3 mm and an outer span, L, of 9 mm at a loading rate of 0.1 mm/min with universal testing machine (AG-25kN, Simadzu, Japan). A miniature load cell (LMA-A-50N-P, Kyowa Instrument Co., Japan) was used to monitor load during bending tests. A strain gauge with 0.2 mm gauge length (KFG02-120, Kyowa Instrument Co., Japan) was glued on the compressive surface to monitor bending strain during the bending tests. Bending stress, σ_B was calculated as

$$\sigma_B = \frac{3P(L-l)}{2wt^2}, \tag{1}$$

where P denotes the load and w and t are specimen width and thickness, respectively. In order to characterize strength data statistically, we used Weibull type distribution as

$$F = 1 - \exp\left(-\left(\frac{\sigma}{\sigma_0}\right)^m\right) \tag{2}$$

where F, σ, m and σ_0 denote fracture probability, strength, shape parameter and scale parameter. In the present study, shape parameter, m, was used as the degree of the dispersion of strength. Bending modulus was calculated from the slope of the bending stress-bending strain curves.

Fracture toughness measurements were also conducted with indentation method using micro-Vickers hardness testing machine (MVK-G2000, Akashi Co., Japan). Fracture toughness K_{IC} were calculated based on the median crack equation as

$$K_{IC} = 0.018\left(\frac{E}{HV}\right)^{0.5}\left(\frac{F}{C^{1.5}}\right) = 0.026(E \cdot F)^{0.5}\frac{a}{C^{1.5}} \quad (3)$$

where F denotes the indentation load, E denotes Young's modulus, HV denotes the Vickers Hardness, C is half of the radial crack length and a is half of the average indent diagonal. Test load of 200 gf with a holding time of 10 s was used in the present investigation. Ten measurements were conducted on each specimen to give the average value.

3 Results and discussion

Figure 3 shows the relative density of the sintered compacts. Average values and standard deviations are shown. Theoretical density of HA was assumed to be 3.16 g/cm^3, which is calculated with the experimentally obtained lattice constants [10]. The relative density becomes larger with increasing pressure from 7.81 MPa to 31.2 MPa. At the pressure larger than 31.2 MPa, the relative density becomes constant value of 96%. The standard deviation of density also became smaller.

The bending strength and fracture toughness as a function of the sintering pressure are shown in Figs. 4 and 5, respectively. Average values and standard deviations are shown. The variation in the bending strength with sintering pressure is similar to fracture toughness. That is, the bending strength and the fracture toughness become smaller with increasing sintering pressure. Especially, bending strength decreases drastically in the specimen sintered at the pressure larger than 31.2 MPa, at which the relative density of the sintered compacts becomes 96%.

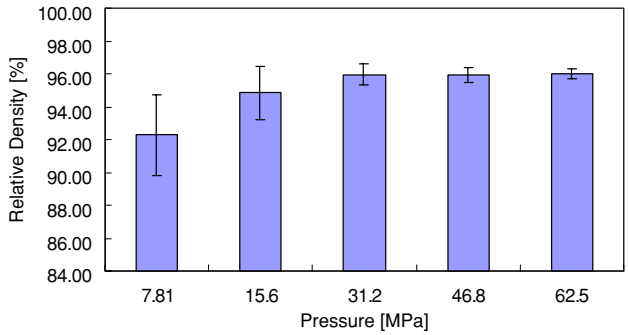

Fig. 3 Relative density of HA with sintering pressure.

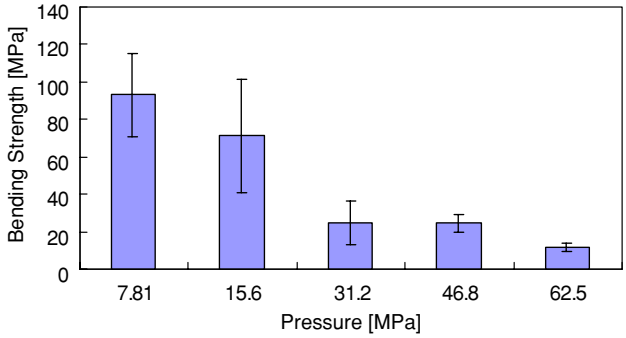

Fig. 4 Bending strength of HA with sintering pressure.

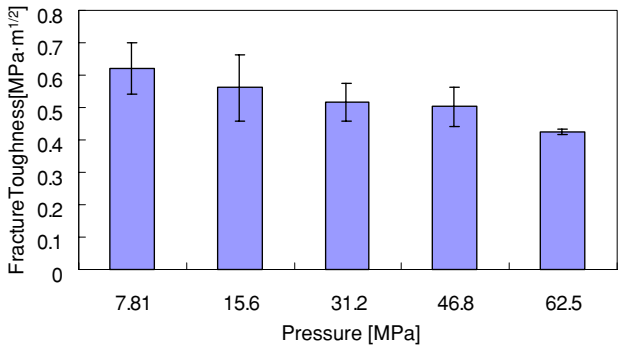

Fig. 5 Fracture toughness of HA with sintering pressure.

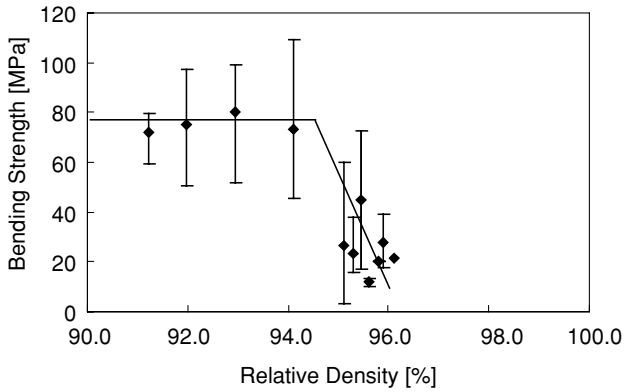

Fig. 6 Bending Strength as a function of Relative Density.

To discuss the quantitative relation between the mechanical properties and the density, the bending strength and the fracture toughness as a function of the relative density are shown in Figs. 6 and 7, respectively. Solid symbol means an average value at each relative density. The range in strength and toughness means maximum and minimum values. The bending strength of HA with relative density <94% is constant in spite of scattering in the values. Then, the strength becomes 40% at the relative density >95%. Fracture toughness also decreases at the density >95%. Figure 8 shows the relation between Weibull shape parameter and relative density. Shape parameter significantly decreases at the density >94%. This means the dispersion of strength becomes larger at the density >94%.

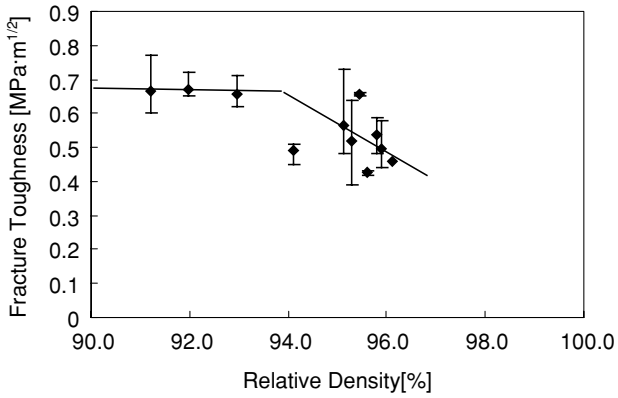

Fig. 7 Fracture Toughness as a function of Relative Density.

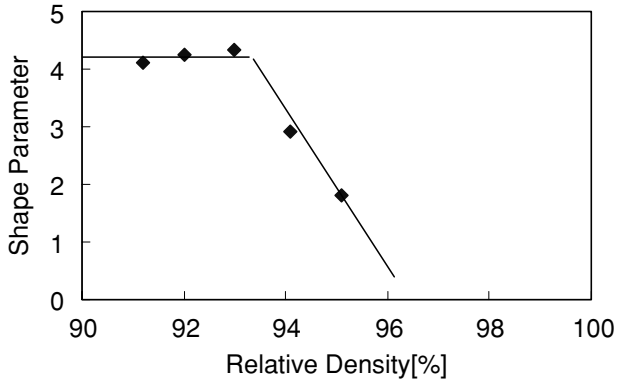

Fig. 8 Weibull shape parameter as a function of relative density.

The reasons of both significant decrease in strength and toughness and significant scattering in strength are considered as the grain growth, decomposition of HA and/or residual stress. The surface observation results in Fig. 9 indicates that the grain growth do not occur during sintering process. At the temperature higher than 850°C, dehydroxylation of HA occurs [11] as

$$Ca_{10}(PO_4)_6(OH)_2 \rightarrow 2Ca_3(PO_4)_2 + Ca_4P_2O_9 + H_2O \quad (4)$$

That is, secondary phases of tricalcium phosphate and tetracalcium phosphate become the initial flaws. To evaluate the decomposition of HA, X-ray diffraction (XRD) analysis was conducted. Figure 10 shows XRD patterns of HA with relative density of 91.2% and 95.9%. The peaks becomes broad in HA with the relative density of 95.9%, which means a little reduction in the crystallization of HA occurred. From this result, it is confirmed that mechanical loading slightly accelerates dehydroxylation.

During sintering process, residual stress is considered to become larger with increasing sintering pressure. From the result of Fig. 9, peak shift was also observed in HA with the relative density of 95.9%. This corresponds to the existence of residual strain. That is, the residual stress is induced in the HA. From the present study, it is clarified that strength and toughness reduction is mainly due to the decomposition and the residual stress.

Figure 11 shows the bending modulus as a function of the relative density. In the range of the relative density of HA obtained in the present study, the bending modulus linearly increases with increasing relative density. In Fig. 10, analytical prediction based on micromechanics [12–14] is also shown. Modulus, E is calculated based on the following equation,

$$E = \frac{E_0}{1 + \frac{3f(1-\nu)(9+5\nu)}{2(1-f)(7-5\nu)}} \quad (5)$$

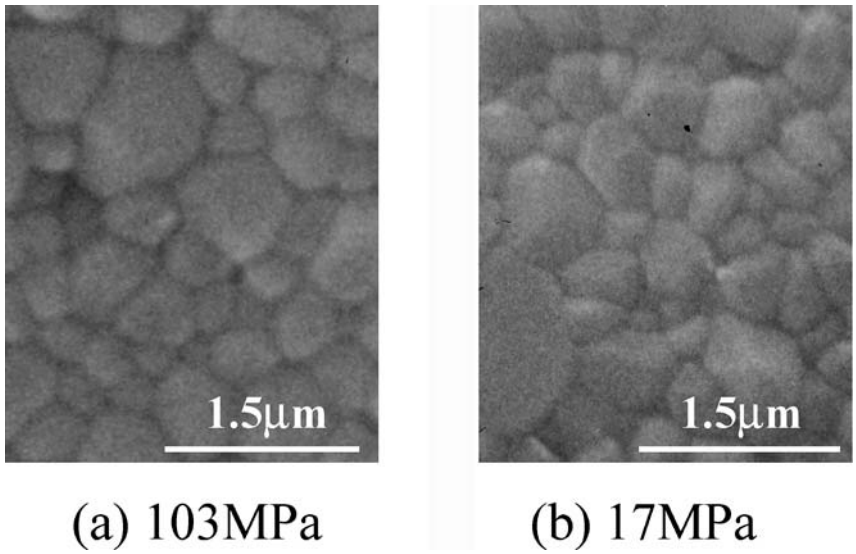

Fig. 9 Scanning electron micrographs of HA. ((a) Bending strength: 103 MPa and (b) Bending strength: 17 MPa).

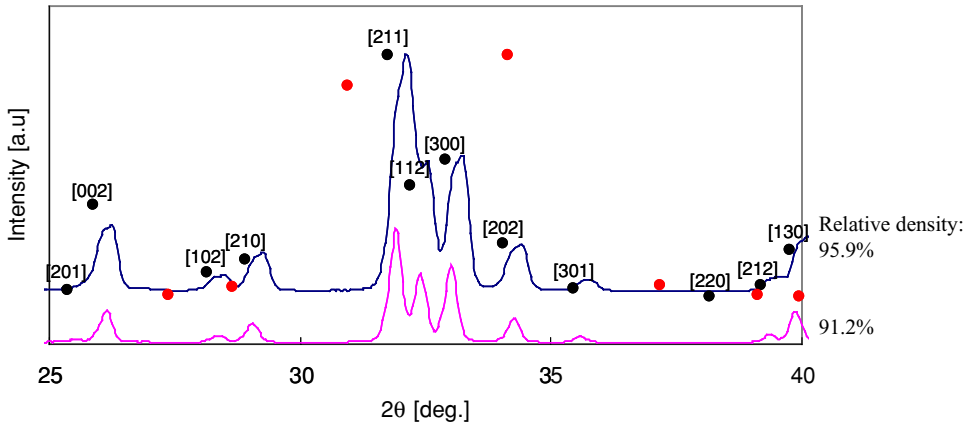

Fig. 10 X-ray diffraction pattern of HA (Relative density: 91.2%, Bending strength: 82.2 MPa, Sintering pressure: 7.81 MPa and Relative density: 95.9%, Bending strength: 24.6 MPa, Sintering pressure: 46.8 MPa).

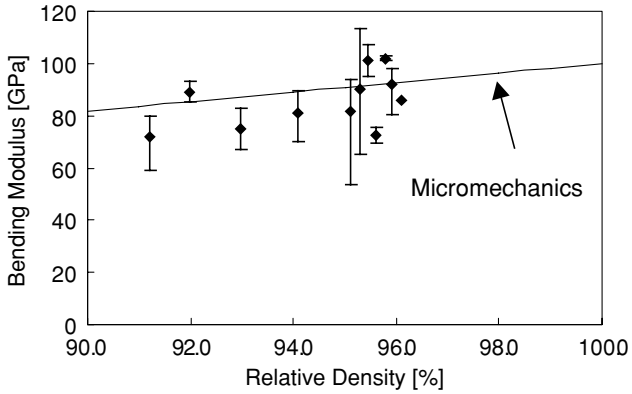

Fig. 11 Bending modulus as a function of Relative Density (Experimental result and analytical prediction).

where E_0 is the modulus with the relative density of 100%, f is porosity and ν is Poisson's ratio. In the present analysis, E_0 and ν are assumed as 100 GPa and 0.22, respectively. In this relative density range, micromechanical analysis is in good agreement with experimental results. It is proved that this analysis is applicable for hydroxyapatite ceramics. This analysis is useful for optimum material design considering physical biocompatibility based on the degree and/or area of disease.

4 Conclusion

In the present study, the effects of sintering pressure on the mechanical properties of HA were investigated and following conclusions were obtained.

(1) The bending strength and the fracture toughness seriously decrease with the relative density >96%.
(2) The dispersion of strength becomes larger at the density >94%.
(3) The reduction in strength and toughness with high relative density is due to HA decomposition and residual stress.
(4) Micromechanics are useful to predict the variation in modulus with the relative density.

References

1. A. ROYER, J. C. VIGUIE, M. HEUGHEBAERT and J. C. HEUGHEBARERT, *J. Mater. Sci. Mater. Med.* **4** (1993) 76.
2. R. HALOUANI, D. BERNACHE-ASSOLANT, E. CHAMPION and A. ABABOU, *J. Mater. Sci. Mater. Med.* **5** (1994) 563.
3. P. VAN LANDUYT, F. LI, J. P. KEUSTERMANS, J. M. STREYDIO, F. DELANNAY and E. MUNTING, *J. Mater. Sci. Mater. Med.* **6** (1995) 8.
4. A. J. RUYS, M. WEI, C. C. SORRELL, M. R. DICKSON, A. BRANDWOOD and B. K. MILTHORPE, *Biomaterials* **16** (1995) 409.
5. M. A. FANOVICH and J. M. PORTO LÓPEZ, *J. Mater. Sci. Mater. Med.* **9** (1998) 53.
6. G. MURALITHRAN and S. RAMESH, *Ceram. Int.* **26** (2000) 221.
7. N. THANGAMANI, K. CHINNAKALI and F. D. GNANAM, *Ceram. Int.* **28** (2002) 355.
8. L. GUO, M. HUANG and X. ZHANG, *J. Mater. Sci. Mater. Med.* **14** (2003) 817.
9. Y. W. GU, N. H. LOH, K. A. KHOR, S. B. TOR and P. CHEANG, *Biomaterials* **23** (2002) 37.
10. M. I. KAY, R. A. YOUNG and A. S. POSNER, *Nature* **204** (1964) 1050.
11. P. E. WANG and T. K. CHAKI, *J. Mater. Sci. Mater. Med.* **4** (1993) 150.
12. J. D. ESHELBY, *Proc. R. Soc.* **A241** (1957) 376.
13. J. D. ESHELBY, *Proc. R. Soc.* **A252** (1957) 561.
14. T. MORI and K. TANAKA, *Acta. Met.* **21** (1973) 571.